Available online at www.sciencedirect.com
ScienceDirect
Physics Procedia 70 (2015) 707 – 711
Physics Procedia

2015 International Congress on Ultrasonics, 2015 ICU Metz

Imaging AOTFs with low RF power in deep-UV and Mid-IR

S. Valle[a,c,*], J. Ward[a], C. Pannell[b], N. Johnson[c]

[a] *Gooch and Housego (UK) Ltd., Dowlish Ford, Ilminster TA19 0PF, UK*
[b] *8104 Banyan Blvd, Orlando, Fl 32819 USA*
[c] *School of Engineering, Rankine Building, University of Glasgow, Glasgow G12 8LT, UK*

Abstract

Acousto-Optic Tunable Filters (AOTFs) are commonly used for applications where high speed tuning and narrow spectral resolution are required. The RF drive power for peak diffraction efficiency increases as λ^2 and depends on the acousto-optic figure of merit (M_2), which is material dependent. In the VIS-IR region between 450nm and 4.5μm tellurium dioxide (TeO_2) is the common material of choice due to the high M_2. At longer wavelengths (up to about 12μm) the mercurous halides and single crystal tellurium show promise. In both cases the λ^2 dependency dominates the RF power consumption and for wavelengths beyond 3.5μm the RF power consumption is above the practical limit (>5W) for larger aperture AOTF(> 10 mm × 10 mm). In the UV range (200nm − 400nm) the λ^2 dependency is no longer dominant and the power consumption depends mainly on the M_2,however, for most materials transparent in the UV the M_2 is poor and thus the drive power will again be excessive (>5W). In order to reduce the RF power requirement to reach peak diffraction efficiency, a resonant configuration in crystal quartz shows promise, especially in the UV range due to its low acoustic attenuation. We describe an AOTF operating in resonance made of crystal quartz, where the reduction of RF power consumption will be reduced by a factor between 15 and 20 compared to a conventional AOTF, thus reducing the power consumption to be within the practical limit (<5W).

Peer-review under responsibility of the Scientific Committee of ICU 2015

Keywords: AOTF; resonant cavity; Infrared; Ultraviolet;Imaging application

1. Introduction

Acousto-Optic Tunable Filters (AOTFs) are typically the component of choice for applications such as Spectroscopy, Remote Sensing, and Hyper-Spectral Imaging where an agile random-access tunable filter is required. AOTFs are solid-state agile random-access electronically addressable tunable filter, where the centre passband is controlled by the frequency of acoustic waves generated by an ultrasonic transducer bonded to an AO material. Acoustic waves are generated by the acoustic transducer when an RF signal is applied, and the incoming electromagnetic radiation is diffracted when the phase matching condition is satisfied between photons and phonons. The polarization of the diffracted order is rotated by $\pi/2$ due to the AO interaction. There are an infinite number of configurations where the phase matching condition is achieved; in order to maximize the field of view of the device a constraint, known as parallel tangent matching condition, presented by Chang (1974), is applied. Due to the large acceptance angle

* Corresponding author. Tel.: +44(0)1460256440; fax: +44(0)1460256441.
E-mail address: svalle@goochandhousego.com

Peer-review under responsibility of the Scientific Committee of ICU 2015
doi:10.1016/j.phpro.2015.08.096

achievable, this configuration is particularly suitable for imaging applications, submitted by **?**.
The possible wavelength range of the filter is determined by the transmission window of the material and its acousto-optic properties. In the range between 450 nm and 4.5μm the common material of choice is Tellurium Dioxide. In the IR region up to 12μm several materials could be used such as mercorous halide, presented by Knuteson et al. (2006) and single crystal Tellurium, reported by Gupta et al. (2012). In the range from 180 nm to 450 nm crystal quartz or KDP crystals could be used, but the unfavourable AO properties add some limitation in the achievable performance.
Here we have focused on the deep-UV range, which is of particular interest for space imaging application and gas detection. Previous work by Dekemper et al. (2014) reported an imaging AOTF made of KDP, but due to its physical properties particular attention is required during the manufacturing and bonding process. However crystal quartz is a well known material easy to process and available in large good quality bricks, but the relatively poor AO figure of merit for quartz limits the performance of an imaging AOTF, due to the high RF power needed to reach peak diffraction efficiency.

2. Efficiency of the AO interaction

The RF power required to achieve Peak Diffraction Efficiency (PDE) depends on the square of the wavelength and the acousto-optic figure of Merit, defined by Xu et al. (1992):

$$M_2 = \frac{n_i^3(\lambda)n_d^3(\lambda)p_{eff}^2}{\rho V^3} \tag{1}$$

where n_i and n_d are the refractive indexes of the incident and diffracted order and p_{eff} is the effective photoelastic constant. When the phase matching is satisfied the RF power for PDE is evaluated as:

$$P_{PDE} = \frac{\lambda^2 H}{2M_2 L_a} \tag{2}$$

where H is the height of the acoustic transducer and L_a is the interaction length.
In the IR region the λ^2 dependency dominates the RF power consumption, but in the UV region, due to short wavelength P_{PDE} is mainly dependent on the value of M_2. Typical values of acousto-optic figure of merit for different AO materials are reported in table 1, reported by Kim et al. (2007).
A notional limit on the RF power has been set as 5 W, thus PDE is not achievable along the whole transmission range of the AO material. This limit is set to avoid excessive thermal gradients inside the crystal, which will affect the performance of the device, and by the available RF power delivered by our RF amplifier over a broad frequency range.

Table 1. Acousto-optic properties of material from deep-UV to IR

Material	Transparency window (μm)	$M_2 \times 10^{-15}$ s^3/kg	Acoustic Velocity (m/s)
Quartz	0.18 - 3.5	0.2	3510 (SS)
KDP	0.21 - 1.5	3	XX (SS)
TeO_2	0.35 - 4.5	1200	617 (SS)
Hg_2Cl_2	0.4 - 20	1050	347 (SS)
Hg_2Br_2	0.35 - 30	2600	273 (SS)
Te	4 - 20	133333	980(S)

3. Resonant Configuration

The RF power required for peak diffraction is limited by the material properties, therefore the power reduction could be obtained with an optimized design maximizing M_2 and minimizing the ratio H/L_a. In conventional AOTFs the phonons are diverted out of the Bragg plane after the AO interaction takes place.
A reduction of P_{PDE} could be also obtained by “recycling” the phonons by configuring the AOTF as a resonant cavity.

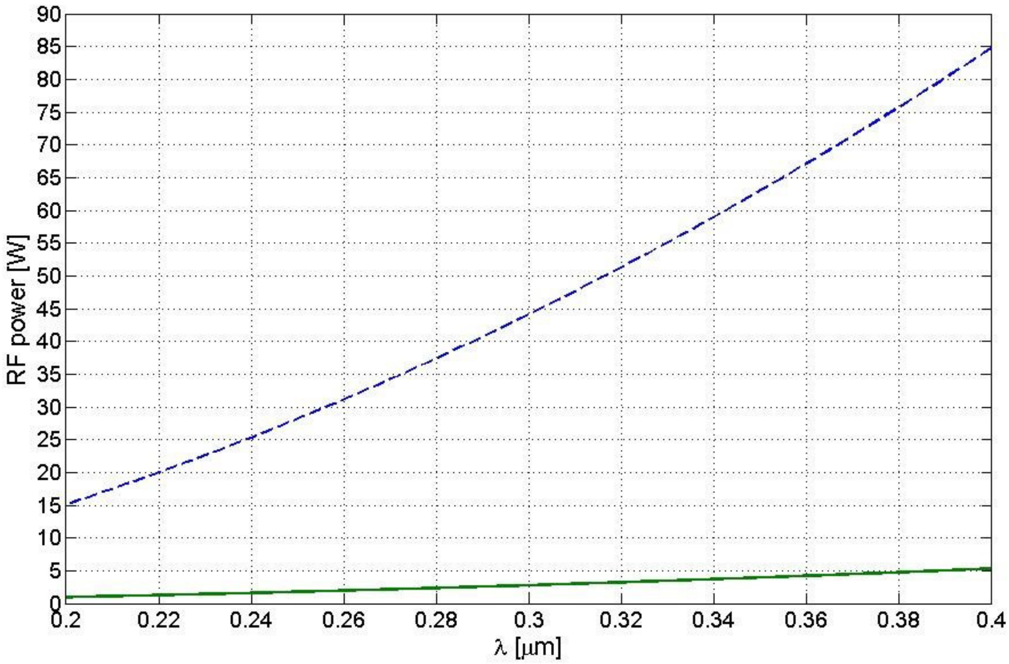

Fig. 1. RF Power to achieve peak diffraction efficiency for the conventional and resonant AOTF

The advantage factor is determined by the acoustic attenuation, which ultimately will depend on the square of the acoustic frequency and also on the acoustic spreading due to diffraction. An optimized design of a TeO_2 AOTF operating between 2μm and 4.5μm has been reported previously by Valle et al. (2015), where due to the elevated acoustic attenuation, it was shown that the resonant configuration is suitable only for the IR region. In the case of crystal quartz the acoustic attenuation is lower and the resonant configuration could be extended to higher frequency. In the resonant cavity, the presence of a travelling wave causes the acoustic energy to be returned to the ultrasonic transducer and this generates a feedback signal which affects the RF coupling when off resonance. The VSWR reaches level over 20, thus the electrical reflection coefficient is equal to 81.9% and practically no acoustic power is coupled inside the AO cell.

In order to stabilize the resonance frequency of the device, a temperature control mechanism is applied using a Peltier heat pump and a digital temperature sensor with a precision of 0.03°C. The same mechanism could be used to move the resonant peak along the wavelength axis by controlling the temperature. This configuration is very effective in quartz due to its high thermal conductivity.

4. Resonant Quartz AOTF

A quartz AOTF in resonant configuration could reduce P_{PDE} theoretically up to 15-20 times, therefore in the spectral region between 180 nm and 400 nm the maximum power is below 5 W (Fig.1). A Quartz AOTF had been designed, built, and tested to verify the principle of the non-collinear configuration with a wavelength range between 400nm and 600nm. The tuning range was selected to match the spectral range of the supercontinuum source (400 nm - 2000 nm) and the optical spectrum analyser available. The acoustic direction is equal to $\theta_a \simeq$ -81° and $\theta_i \simeq$ 17° and the tuning range is between 35 MHz and 55 MHz. The acoustic attenuation had been estimated equal to $\alpha \simeq 0.5$ dB/m. The advantage factor theoretically achievable is between 15-20, therefore the RF power for PDE is theoretically well below 5 W (Fig.2)

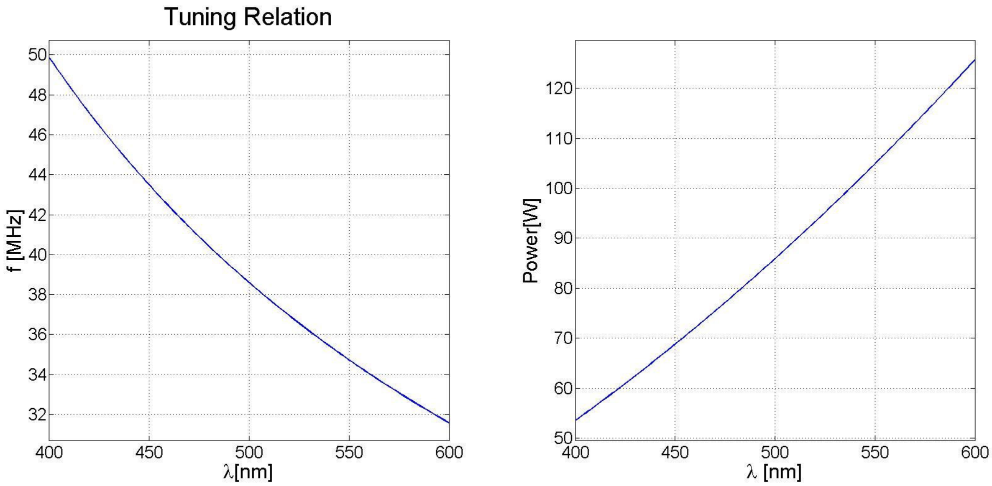

Fig. 2. Tuning relation (left) and RF power for peak diffraction efficiency (right)

The diffraction efficiency versus RF power is usually recorded using a laser line test with a lock-in amplifier configuration. Due to the small separation angle a cross polarization technique was used to separate the diffracted order from the 0^{th} order.

Preliminary results shows an advantage factor equal to 7, the low advantage factor measured on the preliminary results is almost certainly due to the acoustic divergence in Quartz, which has not been investigated yet for this particular design.

5. Conclusion

In conclusion the feasibility of an imaging UV AOTF made of crystal quartz had been shown, the low acousto-optic figure of merit limits the diffraction efficiency achievable, but the resonant configuration looks a promising solution to reduce the acoustic power consumption, due to the low acoustic attenuation in crystal quartz. A first prototype has been built with a tuning range between 400 nm and 600 nm in order to verify the accuracy of the mathematical model developed, which shows an advantage factor of about 7, but more extensive tests are planned in the future to fully characterize the device. An optimized design for the wavelength range between 180 nm and 400 nm is under development with conventional and resonant configuration, with an active aperture over 10 mm × 10 mm. It is expected to reduce the RF power for peak diffraction efficiency below 10 W across the whole range, assuming an advantage factor of approximately 7.

Acknowledgements

The authors thank Gooch and Housego Ltd. for the support, especially Graham Glenn for the helpful advice on the RF matching.

References

I. C. Chang, Noncollinear acousto-optic filter with large angular aperture. Appl. Phys. Lett. 25, pag. 370,oct 1974, DOI:10.1063/1.1655512

David J. Knuteson and Narsingh B. Singh and Milton Gottlieb et al., Crystal growth, fabrication, and design of mercurous bromide acousto-optic tunable filters. Optical Components, Detectors, And Displays. 46, 064001-1 – 064001-5. June 2006. DOI:10.1117/1.2744369

N Gupta, V B Voloshinov, G A Knyazev and L A Kulakova, Tunable wide-angle acousto-optic filter in single-crystal tellurium. Journal of optics, 14, July 2012. DOI:10.1088/2040-8978/14/3/035502

Jieping Xu and Robert Stroud", "*Acousto-Optic Devices*". John Wiley and Sons, Inc., 1992.

Joo-Soo Kim, Sudhir B. Trivedi, Jolanta Soos, Neelam Gupta and Witold Palosz. "Development of mercurous halide crystals for acousto-optic devices". Imaging Spectrometry XII, sep 2007. SPIE, DOI:10.1117/12.734102.

C. N. Pannell and J. D. Ward and E. S. Wachman and B. G. Zhang and M. K. Reed. A high-performance passband-agile hyperspectral imager using a large aperture acousto-optic tuneable filter. Photonic Instrumentation Engineering II, mar 2015. SPIE. "DOI:10.1117/12.2076468"

S. Valle and J. Ward and C. Pannell and N. P. Johnson, Acousto-optic tunable filter for imaging application with high performance in the IR region". Proc. SPIE, 9359. mar 2015, DOI:10.1117/12.2077610

E. Dekemper and D. Fussen and D. Pieroux and J. Vanhamel. Altius: a spaceborne AOTF-based UV-VIS-NIR hyperspectral imager for atmospheric remote sensing. Proc. SPIE 9241, mar 2014, DOI:10.1117/12.2063937